

Films of Metal Nanocrystals Formed at Aqueous–Organic Interfaces[†]

C. N. R. Rao,* G. U. Kulkarni, P. John Thomas, Ved Varun Agrawal, and P. Saravanan

Chemistry and Physics of Materials Unit, Jawaharlal Nehru Center for Advanced Scientific Research, Jakkur, Bangalore 560 064, India

Received: January 3, 2003

Nanocrystalline films of Au, Ag, and Cu have been prepared at the toluene–water interface by the interaction of metal–triphenylphosphine complexes in the organic layer with partially hydrolyzed tetrakis(hydroxymethyl)phosphonium chloride in the aqueous layer. The nanocrystals have been characterized by a host of microscopic and spectroscopic techniques. The free-standing films could be transferred from the interface onto solid supports. Furthermore, films could be dissolved to yield either a hydrosol or an organosol with the help of appropriate surfactants.

Introduction

Nanocrystals of metals such as Au, Ag, Cu, and Pt have been prepared by a variety of methods including the thermal decomposition or controlled reduction of metal salts in constrained environments such as micelles and at the air–water interface.^{1–5} Thus, tiny nanocrystals containing the magic number of 55 Au atoms have been obtained starting with Au(PPh₃)Cl.⁶ The use of AOT–water–isooctane reverse micelles has proven to be a useful method to synthesize metal nanocrystals of controlled dimensions.⁷ Duff et al. elucidated the role of partially hydrolyzed tetrakis(hydroxymethyl)phosphonium chloride (THPC) as a reducing agent in the preparation of Au nanocrystals.^{8,9} Copper nanocrystals in the form of hydrosols are prepared using hydrazine as a reducing agent.¹⁰ High-quality Ag nanocrystals have been prepared by the thermal decomposition of fatty acids of silver.¹¹ A popular method due to Brust et al.¹² involves the use of tetraoctylammonium bromide as a phase-transfer agent to transfer Au³⁺ ions from the aqueous medium to the organic medium prior to reduction. Capping agents such as long-chain alkane thiols are usually added to stabilize the organosol. We have found that metal nanocrystals are readily transferred from the aqueous to the organic layer by first cleansing the nanocrystals and capping them with long-chain thiols. Au, Ag, Pt, and Pd nanocrystals of diameters in the range of 2–8 nm could be transferred from the aqueous to the organic medium by this method.^{13–15}

Nanocrystals anchored to surfaces in the form of a film are considered to be important because of their potential use in nanodevices. It occurred to us that it should be possible to exploit a liquid–liquid interface to synthesize and cast metal nanocrystals into a film in situ. For this purpose, we have made use of two immiscible liquids such as toluene and water, with the metal precursor in the organic layer and the reducing agent in the aqueous layer. By this procedure, we have been able to obtain Au nanocrystals in the form of a film at the interface. We have extended the method to obtain nanocrystals of Ag and Cu as well. This method is to be distinguished from others where the metal nanocrystals synthesized *ex situ* are obtained in the form of films at the air–liquid or liquid–liquid interfaces.^{16–18} Furthermore, the free-standing films obtained by the present



Figure 1. Nanocrystalline film of Au formed at the toluene–water interface (middle). Gold is introduced as a toluene solution of Au(PPh₃)Cl, and partially hydrolyzed THPC (tetrakis(hydroxymethyl)phosphonium chloride) in water acts as a reducing agent. The film is obtained when the two layers are allowed to stand for several hours. When dodecane-thiol is added to the toluene layer, the film breaks up, forming an organosol (left), and mercaptoundecanoic acid added to water produces a hydrosol (right).

method could be converted either to an organosol or to a hydrosol by using appropriate capping agents.

Experimental Section

Au(PPh₃)Cl (Ph, phenyl), Cu(PPh₃)Cl, and Ag₂(PPh₃)₄Cl₂ were prepared by a known procedure.^{19,20} Tetrakis(hydroxymethyl)phosphonium chloride (THPC), dodecane thiol, and octylamine were obtained from Fluka and used without further purification. Mercaptoundecanoic acid (MUA) was obtained from Aldrich. Water used in the experiments was double distilled using a quartz apparatus. In a typical preparation, 10 mL of a 1.5 mM solution of Au(PPh₃)Cl in toluene was allowed to stand in contact with 16 mL of 6.25 mM aqueous alkali in a 100-mL beaker at 300 K. Once the two layers stabilized, 330 μ L of 50 mM THPC was injected into the aqueous layer using a syringe with minimal disturbance to the toluene layer. The onset of reduction was marked by a faint pink coloration of the liquid–liquid interface. The reduction thus initiated was allowed to proceed without disturbance for several hours. With the passage of time, the color became more vivid, finally resulting in a robust elastic film at the liquid–liquid interface (Figure 1). Films of Ag and Cu were prepared by a similar procedure using Ag₂(PPh₃)₄Cl₂ and Cu(PPh₃)Cl.

[†] Part of the special issue “Arnim Henglein Festschrift”.

* Corresponding author. E-mail: cnrao@jncasr.ac.in.

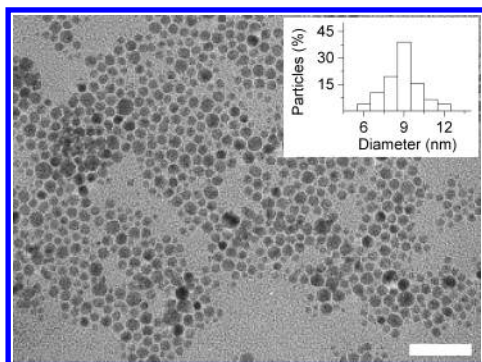


Figure 2. TEM micrograph of the as-prepared standard film obtained after 24 h from a liquid–liquid interface containing a 1.5 mM toluene solution of $\text{Au}(\text{PPh}_3)\text{Cl}$ and $330 \mu\text{L}$ of 50 mM THPC in 16 mL of a 6.25 mM aqueous NaOH solution. The scale bar corresponds to 50 nm. The inset shows a histogram of the diameter distribution obtained from a few hundred particles.

The nanocrystalline films at the interface were characterized by transmission electron microscopy (TEM), UV–vis spectroscopy, atomic force microscopy (AFM), and X-ray photoelectron spectroscopy (XPS). Samples for TEM were obtained by piercing the film with a holey copper–carbon grid from above and gently lifting it along with a tiny portion of the film, following which it was washed with toluene. A JEOL 3010 transmission electron microscope operating at 300 kV was employed for TEM studies. Samples for UV–vis spectroscopy were obtained with a Perkin-Elmer Lambda 900 spectrometer by transferring the film onto a synthetic quartz substrate using the above procedure. Samples for AFM consisted of films transferred by the above procedure on a clean Si(100) surface. Tapping-mode AFM images were obtained using a multimode scanner from Digital Instruments operated with a Nanoscope IV controller. Both the amplitude and the phase images were simultaneously acquired. Standard etched Si cantilevers were used for this purpose. Samples for XPS were prepared by transferring the films onto graphite substrates. XPS was carried out with an ESCALAB MK-IV spectrometer equipped with an Al $K\alpha$ (1486.6 eV) source. The binding energies reported here are referenced to the C(1s) level at 284 eV.

With the addition of a few micromoles of capping agents such as dodecanethiol or octylamine to the toluene layer, the Au film at the interface disappeared within minutes, accompanied by a distinctive pink coloration in the top layer (Figure 1) that is characteristic of an Au organosol. Similarly, the addition of a few micromoles of MUA to the aqueous solution results in the complete dissolution of the film after a few hours and the transfer of its contents to the aqueous layer (Figure 1). The sols thus obtained were characterized by TEM and UV–vis spectroscopy. Samples for TEM were prepared by depositing a few drops of the sols on a holey-carbon-coated copper grid and allowing them to evaporate overnight in a desiccator.

Results and Discussion

Films of Au Nanocrystals. In Figure 2, we show a TEM image of an as-prepared film of Au nanocrystals that was obtained after maintaining the organic–aqueous interface with the reactants for 24 h. The as-prepared film consists of nanocrystals with diameters in the range of 5.5 to 14 nm with a mean of ~ 9 nm. The nanocrystals are present in a close-packed arrangement with a typical interparticle distance of 1.5 nm. A lower-magnification image revealed that the film essentially consists of a monolayer of nanocrystals with high coverage

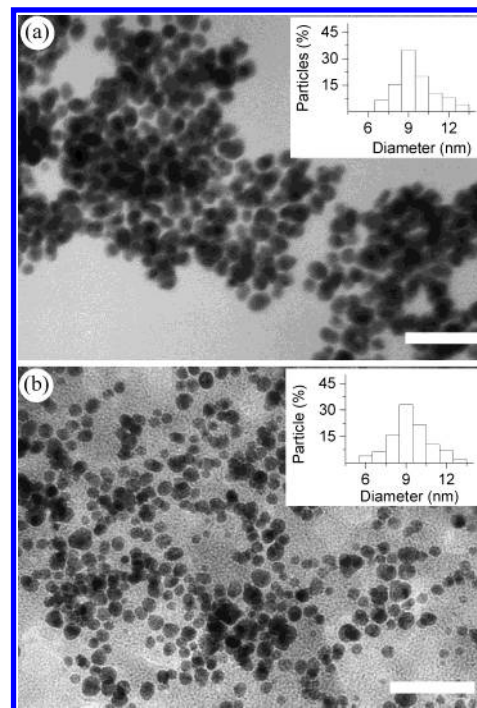


Figure 3. TEM micrographs of (a) dodecanethiol-capped nanocrystals in the organosol and (b) mercaptoundecanoic acid-capped nanocrystals in the hydrosol. The scale bar corresponds to 50 nm. The insets show histograms of the diameter distribution obtained from a few hundred particles in each case.

(>75%). Aggregates and multilayered films were seen in a few areas of the grid. The organosol and the hydrosol also consist of nanocrystals with similar average diameters but with a somewhat wider size distribution, as can be seen from Figure 3a and b. A number of multiply twinned particles are also present in these cases. The close packing of nanocrystals present in the film is not seen in the images in Figure 3a and b.

The nature of the emerging film was examined by systematically varying factors such as the contact time at the interface, the relative amounts of reducing agents, and the Au precursor. In Figure 4, we show the TEM images of the films sampled after contact times of 3, 6, and 9 h. These images may be compared with that of the standard film shown in Figure 2 corresponding to a contact time of 24 h. Clearly, an increase in contact time increases the coverage of the film on the substrate, with no observable change in the average diameter of the nanocrystals. Although a more detailed study on the growth of nanocrystals is essential, our observations seem to suggest that particle growth reaches saturation with time while fresh nucleation sites are constantly being created.

The use of high concentrations of the reducing agent results in less-uniform films with altered distributions in the particle diameter, as can be seen from a comparison of Figure 5 with Figure 2. When the concentration of THPC was doubled, the distribution was somewhat narrower with an average diameter of ~ 9.5 nm (Figure 5a). A further increase in the concentration of the reducing agent results in broader distributions in diameters (Figure 5b). We notice that the close packing of the particles seen in Figure 2 is lost at higher concentrations of the reducing agent. The films formed at higher concentrations of the reducing agent also exhibit a distinct tendency to form multilayers. However, when the concentrations of the Au precursor and reducing agent were increased simultaneously, the film primarily consisted of a monolayer of nanocrystals with a broader size distribution and a higher coverage (Figure 6). The broader

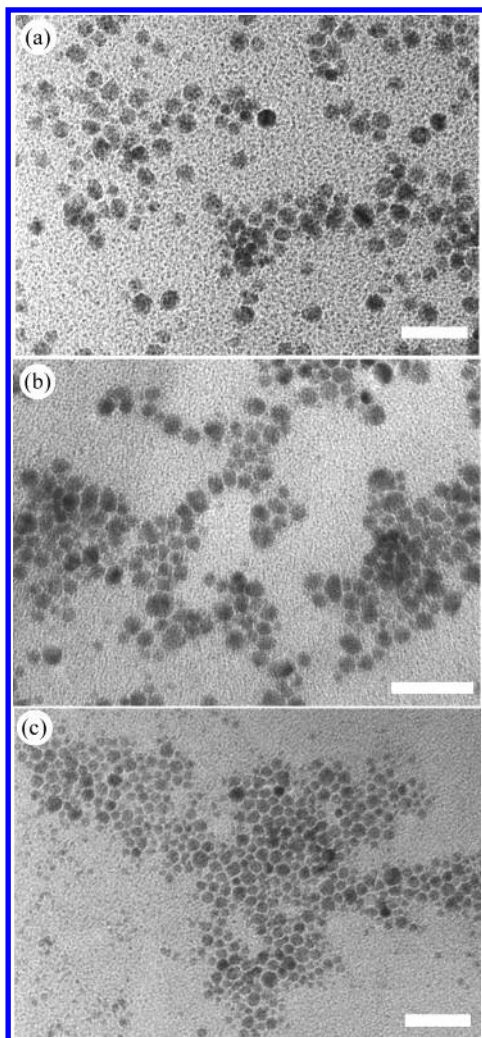


Figure 4. TEM micrographs of the films collected from a liquid–liquid interface containing a 1.5 mM toluene solution of Au(PPh₃)Cl and 330 μ L of 50 mM THPC in 16 mL of a 6.25 mM aqueous NaOH solution with different contact times: (a) 3, (b) 6, and (c) 9 h. The scale bars in all cases correspond to 50 nm.

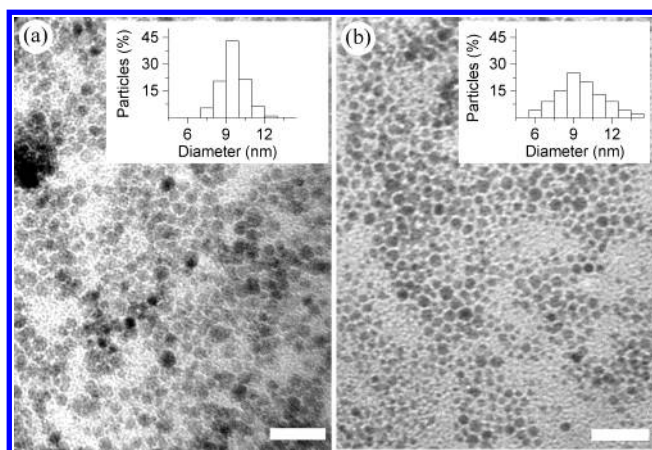


Figure 5. TEM micrographs of films collected after 24 h from a liquid–liquid interface containing a 1.5 mM toluene solution of Au(PPh₃)Cl and 16 mL of a 6.25 mM aqueous NaOH solution with (a) 660 and (b) 1200 μ L of 50 mM THPC. The concentrations correspond to metal/reducing agent ratios of 1:2 and 1:4, respectively. The scale bars correspond to 50 nm. The insets show histograms of the diameter distribution obtained from a few hundred particles in each case.

distribution hinders the formation of the close-packed arrangement of nanocrystals.

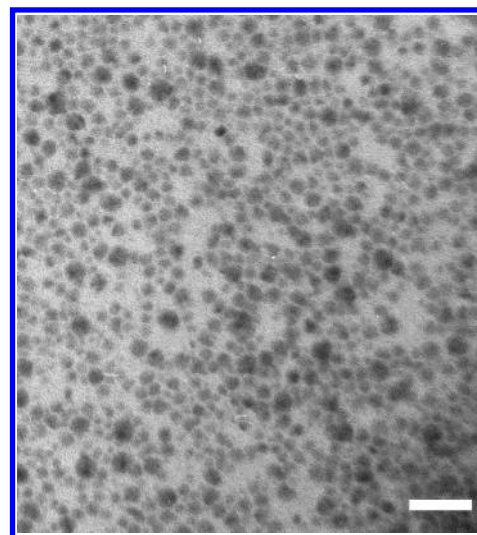


Figure 6. TEM micrograph of the film collected after 24 h from a liquid–liquid interface containing a 7.5 mM toluene solution of Au(PPh₃)Cl and 16 mL of a 31.25 mM aqueous NaOH solution with 1650 μ L of 50 mM THPC. The concentrations of the reactants are, therefore, 5 times the usual concentration. The scale bar corresponds to 50 nm.

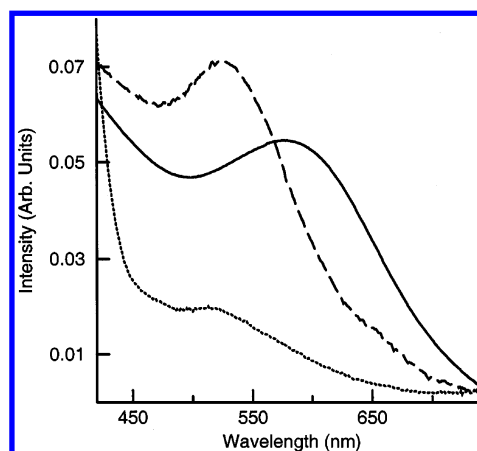


Figure 7. UV–vis spectra of the as-prepared standard film on a synthetic quartz substrate (—), octylamine-capped nanocrystals in toluene (---), and mercaptoundecanoic acid-capped nanocrystals in water (··).

The choice of ingredients deserves to be mentioned. It seems to be important that the right choice of metal precursor and reducing agent is employed to obtain stable films at the liquid–liquid interface. For instance, Au³⁺ ions complexed with tetraoctylammonium bromide in toluene did not form a film at the interface but yielded an organosol. Similarly, more powerful reducing agents such as sodium borohydride fail to produce uniform nanocrystalline films. The choice of organic solvent also seems to be important. Although we were able to obtain stable films with benzene and dichloromethane, solvents such as octanol were a deterrent to film formation.

UV–vis spectra of the as-prepared Au film as well as of the hydrosol and organosol are shown in Figure 7. All of the spectra exhibit bands due to the surface plasmon, the position and intensity depending on several factors such as the diameter of the nanocrystals, the nature of the ligand, and the refractive index of the surrounding medium.^{21,22} The film on a quartz substrate exhibits a broad band centered at 575 nm, and the sols show plasmon bands at \sim 530 nm. The band due to the octylamine-capped nanocrystals (organosol) is more intense compared to that of the MUA-capped nanocrystals from the hydrosol probably because of a dampening of the surface plasmon by

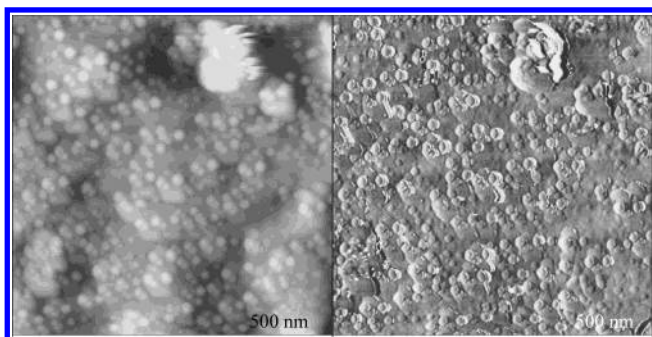


Figure 8. AFM images of the as-prepared film in the tapping mode: (left) amplitude and (right) phase imaging.

the thiol. The higher wavelength of the plasmon band of the film could be due to the relatively higher dielectric constant of the surrounding medium.

Tapping-mode AFM images of the as-prepared Au film reveal several features that are mostly spherical in nature (Figure 8) with diameters between 7 and 16 nm, which are somewhat higher than those from the TEM measurements. It is therefore possible that the nanocrystals consist of a layer of the organic ligand, which is invisible in the TEM measurements.^{23,24} AFM images also reveal regions where the nanocrystals are aggregated. Wider scans covering a few micrometers yielded a rms roughness of ~ 35 nm with a maximum peak-to-valley distance of 80 nm. An image acquired at the edge that the film shared with the substrate revealed the thickness of the film to be ~ 60 nm. The surface composition of the film was probed using core-level XPS. The Au(4f) spectra showed a broad doublet, which could be fitted to two Au species with $4f_{7/2}$ binding energies of 84 and 85.2 eV. This is consistent with the picture of a metallic core surrounded by a layer of Au atoms bound to the capping agents.²⁵ The latter may consist of triphenylphosphine ligands and ionic species from THPC. The spectrum revealed the presence of phosphorus and chlorine in the film.

Films of Ag and Cu Nanocrystals. By using $\text{Ag}_2(\text{PPh}_3)_4\text{-Cl}_2$ instead of $\text{Au}(\text{PPh}_3)\text{Cl}$, films of nanocrystalline Ag were obtained. The Ag films exhibited high metallic luster. TEM and AFM images of the film in Figure 9 show nanocrystals with average diameters of 10 and 12 nm, respectively, the difference mainly arising from the surface ligands. The film is primarily a nanocrystalline monolayer with high coverage ($\sim 70\%$). XPS measurements revealed the presence of two Ag species, one due to the core of the nanocrystal and the other due to Ag bound to the capping agent. Furthermore, no evidence of the oxidation of Ag, commonly seen in Ag nanocrystals, was apparent.²⁶ Films of Ag nanocrystals show the characteristic plasmon band at ~ 410 nm.²²

By using $\text{Cu}(\text{PPh}_3)\text{Cl}$ and with only NaOH in the aqueous layer, we could obtain films of Cu nanocrystals. However, the film was not uniform and revealed nanocrystals with a broad distribution of diameters (Figure 10). The film exhibits the red-brown luster characteristic of copper, although one cannot be entirely certain that it consists of only metallic Cu because many Cu suboxides also show such luster. XPS measurements indicated the presence of metallic Cu with a very small proportion of oxide species.

The free-standing nanocrystalline films of Au, Ag, and Cu can be lent some extra strength with the help of solid supports that may also contribute additional properties. The use of a polystyrene support, for example, yields flexible and transparent films. We found that a few drops of a toluene dispersion of the

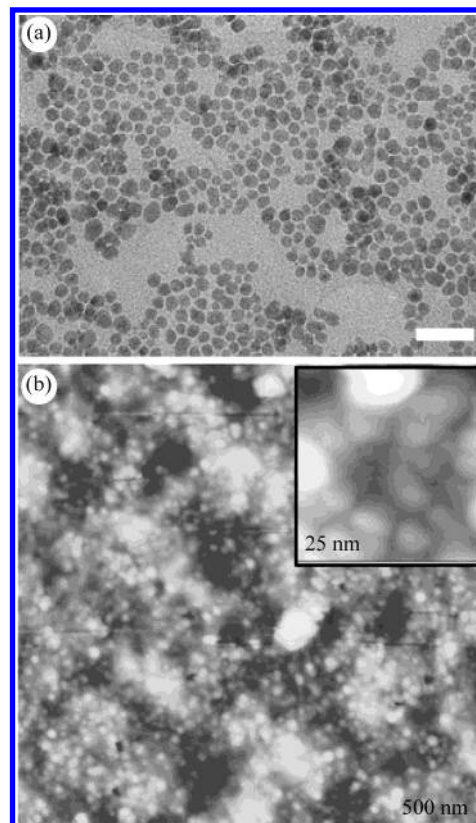


Figure 9. (a) TEM micrograph of a Ag nanocrystalline film. The scale bar corresponds to 50 nm. (b) Tapping atomic force image of the film in the amplitude mode. The inset contains a higher-resolution image showing individual nanocrystals.

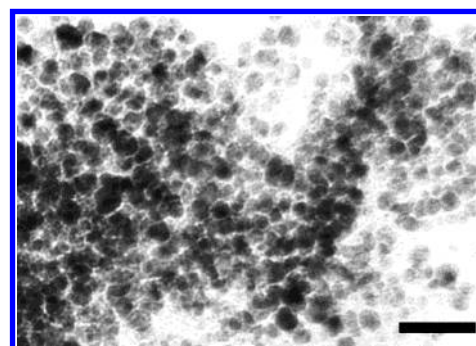


Figure 10. TEM micrographs of Cu nanocrystalline films. The scale bar corresponds to 50 nm.

polymer added to the layer atop the interface yielded the desired film upon the evaporation of the solvent. The film thus obtained was continuous and contained a high density of nanocrystals. We envisage several potential applications of such films in color filters and radiation shields.

Conclusions

The preparation of films of nanocrystals of Au, Ag, and Cu at the liquid–liquid interface has been accomplished by taking a metallo-organic precursor in the organic layer and the appropriate reducing agent in the aqueous layer. The particle diameters and the film coverage are dependent on the contact time and the concentration of the reactants. The films show surface plasmon bands characteristic of metal nanocrystals. The nanocrystals in the films are readily extracted to aqueous or organic layers by adding suitable capping agents. A particularly noteworthy aspect of the study is that the nanocrystalline film at the interface can be easily transferred onto a solid support.

Acknowledgment. P.S. thanks DMSRDE (Kanpur) for a leave of absence.

References and Notes

- (1) Shipway, N.; Katz, E.; Willner, I. *ChemPhysChem* **2000**, *1*, 18.
- (2) *Nanoparticles and Nanostructured Films*; Fendler, J. H., Ed.; Wiley-VCH: Weinheim, Germany, 1998.
- (3) *Clusters and Colloids: From Theory to Applications*; Schmid, G., Ed.; VCH: Weinheim, Germany, 1994.
- (4) Rao, C. N. R.; Kulkarni, G. U.; Thomas, P. J.; Edwards, P. P. *Chem. Soc. Rev.* **2000**, *29*, 27. Rao, C. N. R.; Kulkarni, G. U.; Thomas, P. J.; Edwards, P. P. *Chem.—Eur. J.* **2002**, *8*, 28.
- (5) Yi, K. C.; Hörvölgyi, Z.; Fendler, J. H. *J. Phys. Chem.* **1994**, *98*, 3872.
- (6) Schmid, G. *Inorg. Synth.* **1990**, *7*, 214.
- (7) Pileni, M. P. *J. Phys. Chem.* **1993**, *97*, 6961.
- (8) Duff, D. G.; Baiker, A.; Edwards, P. P. *Langmuir* **1993**, *9*, 2301.
- (9) Duff, D. G.; Baiker, A.; Gameson, I.; Edwards, P. P. *Langmuir* **1993**, *9*, 2310.
- (10) Curtis, A. C.; Duff, D. G.; Edwards, P. P.; Jefferson, D. A.; Johnson, B. F. G.; Kirkland, A. I.; Wallace, A. S. *Angew. Chem., Int. Ed. Engl.* **1988**, *27*, 1530.
- (11) Abe, K.; Hanada, T.; Yoshida, Y.; Tanigaki, N.; Takiguchi, H.; Nagasawa, H.; Nakamoto, M.; Yamaguchi T.; Yase, K. *Thin Solid Films* **1998**, *327–329*, 524.
- (12) Brust, M.; Walker, M.; Bethell, D.; Schiffrin, J. D.; Whyman, R. *J. Chem. Soc., Chem. Commun.* **1994**, 801.
- (13) Sarathy, K. V.; Raina, G.; Yadav, R. T.; Kulkarni, G. U.; Rao, C. N. R. *J. Phys. Chem. B* **1997**, *101*, 9876.
- (14) Sarathy, K. V.; Kulkarni, G. U.; Rao, C. N. R. *Chem. Commun.* **1997**, 537.
- (15) Thomas, P. J.; Kulkarni, G. U.; Rao, C. N. R. *J. Phys. Chem. B* **2000**, *104*, 8138.
- (16) Kumar, A.; Mandal, S.; Mathew, S. P.; Selvakannan, P. R.; Mandale, A. B.; Chaudhari, R. V.; Sastry, M. *Langmuir* **2002**, *18*, 6478.
- (17) Heath, J. R.; Knobler, C. M.; Leff, D. V. *J. Phys. Chem.* **1997**, *101*, 189.
- (18) Chi, L. F.; Rakers, S.; Hartig, M.; Fuchs, H.; Schmid, G. *Thin Solid Films* **1998**, *327–329*, 520.
- (19) Braunstein, P.; Lehner, H.; Matt, D. *Inorg. Synth.* **1990**, *7*, 218.
- (20) Khan, M.; Oldham, C.; Tuck, D. G. *Can. J. Chem.* **1981**, *59*, 2714.
- (21) Link, S.; El-Sayed, M. A. *J. Phys. Chem. B* **2001**, *105*, 1.
- (22) Mulvaney, P. *Langmuir* **1996**, *12*, 12.
- (23) Schmid, G.; Peschel, S. *New J. Chem.* **1998**, 669.
- (24) Reetz, M. T.; Helbig, W.; Quaiser, S. A.; Stimming, U.; Breuer, N.; Vogel, R. *Science* **1995**, *276*, 367.
- (25) Quinten, M.; Sander, I.; Steiner, P.; Kreibitz, U.; Fauth, K.; Schmid, G. *Z. Phys. D: At., Mol. Clusters* **1991**, *20*, 377.
- (26) Strelow, F.; Henglein, A. *J. Phys. Chem. B* **1995**, *99*, 11834.